



UNIVERSIDADE ESTADUAL DE CAMPINAS
SISTEMA DE BIBLIOTECAS DA UNICAMP
REPOSITÓRIO DA PRODUÇÃO CIENTÍFICA E INTELLECTUAL DA UNICAMP

Versão do arquivo anexado / Version of attached file:

Versão do Editor / Published Version

Mais informações no site da editora / Further information on publisher's website:

<https://link.springer.com/article/10.1007/s40430-018-1396-x>

DOI: 10.1007/s40430-018-1396-x

Direitos autorais / Publisher's copyright statement:

©2018 by Springer. All rights reserved.

DIRETORIA DE TRATAMENTO DA INFORMAÇÃO

Cidade Universitária Zeferino Vaz Barão Geraldo

CEP 13083-970 – Campinas SP

Fone: (19) 3521-6493

<http://www.repositorio.unicamp.br>



Kinematics of a variable stroke and compression ratio mechanism of an internal combustion engine

Caio H. Rufino¹ · Janito V. Ferreira¹

Received: 21 May 2018 / Accepted: 3 September 2018 / Published online: 11 September 2018
© The Brazilian Society of Mechanical Sciences and Engineering 2018

Abstract

The development of automotive propulsion has been guided in recent years by policies for the reduction of pollutant emissions. To comply with the imposed regulations, engine adaptability is one of the most effective strategies for meeting efficiency requirements in the case of the diverse operational conditions found in urban traffic. A variable stroke and compression ratio engine is the solution to this requirement. In addition to its advantages, its design inevitably increases the engine's complexity. Thus, it is necessary to conduct studies on the feasibility of such a technology. This work describes a variable stroke and compression ratio engine mechanism and presents a developed kinematic model that is used to evaluate the requirements for the implementation of this mechanism. The results of the evaluation confirm the possibility of using this alternative mechanism to obtain a higher efficiency in internal combustion engines.

Keywords Internal combustion engine · Variable compression ratio · Variable stroke engine · Kinematics of multi-link mechanisms · Flexfuel engines

1 Introduction

The existing environmental issues and health concern in urban centers have resulted in an increase in the amount of attention focused on the development of thermal machines. Most part of urban pollution is emitted by LDV (light-duty vehicles) [3]. The development of the LDV presents a challenge for the automotive industry as an engine for this application is required to be able to work efficiently in urban traffic conditions. The wide variability in the duty of the engine results in the necessity of a machine capable of adapting itself to each condition of operation, which includes speed, load, acceleration, and deceleration, and yet be capable of a quick cold start and stable idle operation.

As the ability of the engine to adapt to its operating conditions improves, its complexity also increases. One strategy that has been recently explored is the VCR (variable compression ratio). The compression ratio is a parameter that is theoretically linked to the thermal efficiency of the engine (Fig. 1). Furthermore, higher values of compression ratio benefit the combustion by increasing the flame speed and consequently reducing the combustion duration [7]. However, the supersonic auto-ignition, known as the knock phenomenon, limits the compression ratio in spark-ignition engines. The conditions in which the knock is critical are related to the induction time of the auto-ignition, i.e., when the air–fuel mixture is exposed to a high pressure and high temperature for a period of time that is sufficient for auto-ignition to occur. This condition becomes more feasible at low speeds. Furthermore, when the engine is running at full load, the amount of mass that is admitted into the cylinder is sufficient to cause an increase in pressure, which in turn results in a dramatic decrease in the induction time of the auto-ignition, thus leading to the knock phenomenon. Therefore, the full-load and low-speed conditions limit the compression ratio. As a consequence, the engine runs away from the conditions of knock at partial loads and/or high speeds. Moreover, VCR technologies would be convenient for multi-fuel engines. This type of engine is very common

Technical Editor: Jose A. R. Parise.

✉ Caio H. Rufino
rufino119186@gmail.com

Janito V. Ferreira
janito@fem.unicamp.br

¹ Laboratory of Biofuel Engines, Department of Computational Mechanics, School of Mechanical Engineering, University of Campinas, Campinas, SP 13083-970, Brazil

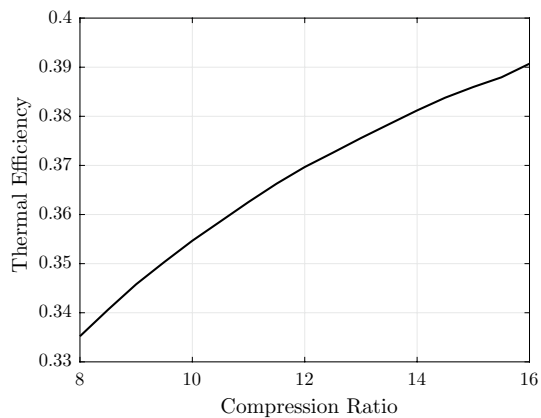


Fig. 1 Effect of the compression ratio on thermal efficiency (adapted from [5])

in Brazil and was implemented in up to 90% of the vehicles sold until 2011 [11]. This flexfuel engine operates with hydrous ethanol, gasohol (gasoline with a 27% volume of anhydrous ethanol as an anti-knock agent, which is a commonly adopted fuel in Brazil), or a mixture of any proportion of both fuels. However, ethanol has characteristics that are different from gasoline and has a higher heat of vaporization, which requires a higher compression ratio for a more complete burn, while gasoline has a lower octane number (value related to sensitivity to auto-ignition), thus requiring a lower compression ratio. As a consequence, flexfuel engines with an intermediate compression ratio are produced, which operate with a low efficiency when fueled with ethanol working at a lower compression ratio than necessary and when fueled with gasoline by retarding the spark-at-knock condition that occurs a greater number of operating conditions. By adjusting compression ratio, the engine could operate at the ideal compression ratio according to the fuel being used.

Other solutions that promise an increase in efficiency in the case of partial loads include the reduction of the throttle operation by limiting the power output by other means. The main motivation is to avoid the pump work that arises when the engine operates at partial loads. When the throttle is not in the fully open position, it generates a pressure drop in the intake manifold, which leads to a high pumping work, thus resulting in a decrease in thermal efficiency. One strategy that mitigates pump losses is controlling the power output by reducing the cubic capacity. This adjustment is done by changing the stroke length of the piston, and this engine is known as a VSE (variable stroke engine). This reduction in stroke length results in not only advantages in the form of a reduction in work by preventing the occurrence of pump losses but also an increase in the mechanical efficiency due to a decrease in the piston's friction [1].

An interesting proposal is the use of a VSE with a VCR comprising a multi-link mechanism [2]. Some preliminary

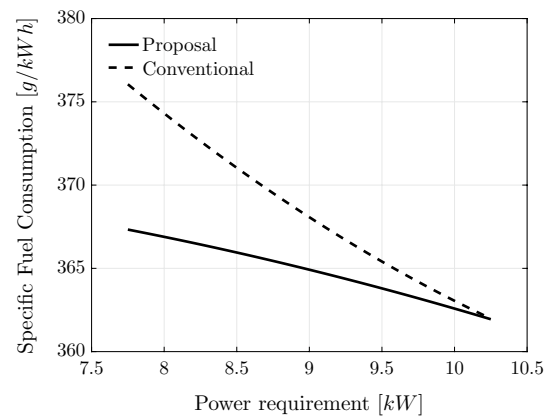


Fig. 2 Comparison of specific fuel consumption results between a conventional engine and the proposed engine (adapted from [5])

results were shown in [5] that explored the fuel economy potential of such an engine. By setting the compression ratio and spark advance as constants, a gain in fuel economy is observed (Fig. 2). A study of how this fuel economy can be improved by combining the adjustment of cubic capacity in parallel with that of the compression ratio with the engine operating at the MBT would be interesting. The initial simulations indicated an expected increase of around 20% in thermal efficiency.

To perform further evaluations of the aforementioned technology [2], this paper establishes relations of the VSE mechanism—which were studied in [5]—that will be implemented in a thermodynamic model for predicting the performance of the proposed engine. The laws of motion for the mechanism are developed. A strategy is also presented for determining the mechanism behavior as a function of a desired set of values of the compression ratio and cubic capacity. In addition, a comparison of the kinematics characteristics is performed between the new mechanism and the conventional one. The objective of this comparison is to indicate the changes in the motion of the piston that results from the implementation of the novel mechanism. This work will be detailed into the description of the mechanism, presentation of the strategy for controlling the stroke length and compression ratio, and the components of the mechanism. The methodology adopted for mapping and developing a relation between the input parameters and the configuration of the components is then presented. Subsequently, the kinematics of the mechanism and its comparison with a conventional engine are exposed. Finally, the concluding remarks are presented, and the scope for future works is described.

2 Description of the mechanism

It was mentioned previously that the redesign of the engine and its components comprise the challenge of the development of a VSE. Siegla and Siewert [8] state that a VSE should ideally provide the capacity for varying the stroke

length without adding weight, volume, and mechanical losses due to friction. However, the design of a minimalist mechanism that allows real-time control over the piston's kinematics is not a trivial task. Any mechanism that is aimed at improvement in operational adaptability will present a greater complexity and a higher number of components as compared to the simple crank-rod mechanism used in conventional engines. Although the addition of components appears to be a contradiction to the downsizing trend in the automotive industry, the increase in efficiency justifies the use of smaller engines, thus compensating for the increase in components.

The stroke–bore ratio is a fundamental parameter for the VSE. Siewert [9] presents a study showing that small stroke–bore ratios induce thermal losses. The increase in the area–volume ratio favors heat losses whenever the stroke length is reduced. Furthermore, a decrease in the flame speed was experimentally observed, which resulted in a decrease in thermal efficiency.

In the mechanism proposed in [5], a lever that connects the piston to the crank-rod mechanism is adopted (see Fig. 3). As the position of the pivot of the lever can be altered, the arm length of the lever can be adjusted, and the stroke length is controlled. Furthermore, the inclination of the lever determines the position of the TDC (top dead center), which controls the compression ratio by regulating the clearance volume.

The addition of a lever modifies the kinematics of the piston. Several multi-link mechanisms cause this modification, which alters the velocity and acceleration of the piston around the TDC and bottom dead center (BDC). However, there is no consensus in the literature on how the piston's

kinematics affects the combustion. Hence, we assume that the kinematics of the proposed mechanism is desired to be similar to that of the conventional crank-rod mechanism. This hypothesis is considered as further evaluation of the effects of kinematics on the development of combustion would require a complex multi-dimensional simulation or experimental tests, which are impossible to execute at the present moment since we are still developing a software and a prototype.

It should be noted that there are two actuators for controlling the horizontal and vertical displacement of the pivot as the mechanism has three degrees of freedom. One possible arrangement of the mechanism is pointed out in Fig. 3. We highlight that there are several arrangements of the mechanism for controlling the pivot's displacement. Thus, it is assumed in this study that the pivot position is being defined by an actuation system without detailing the layouts and arrangements of the actuation system.

The piston is pinned to a rod, which does not execute an alternative motion as in the case of conventional mechanisms. As a consequence, the lateral forces that act on the side of the piston's head are absorbed by the rod as it is in direct contact with the crank case (Fig. 3). This characteristic is highlighted as another advantage of the proposed mechanism because the reduction of the lateral forces acting on the piston can increase its durability.

The dimensions defined in this work are that of a prototype that is fabricated and assembled. The dimensions are given in Table 1.

It should be noted that the lever amplifies the motion of the crank-rod mechanism to the piston. This means that the crank radius R must be shorter than the crank radius in the conventional mechanism, thus resulting in a weight reduction estimated on about 35%. We found a weight increase of 80% when comparing the conventional mechanism, formed by piston, connecting rod and crankshaft, with the proposed mechanism, which has the additional parts lever and piston rod. It should be noted that most of this weight increase is due to the adopted mechanism solution that was chosen with the main idea of evaluating the new concept and not with the objective of choosing an

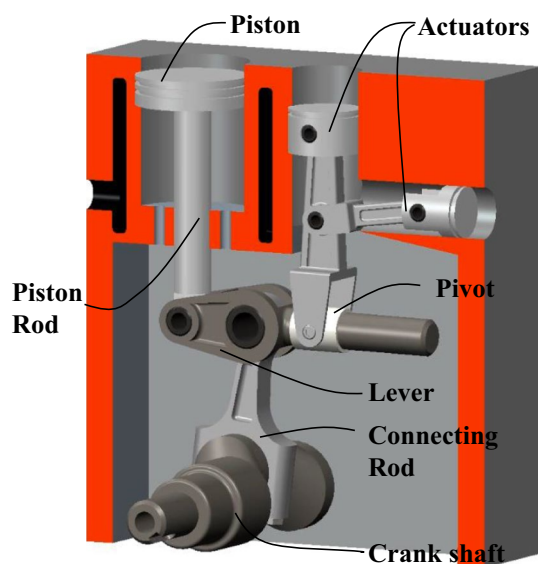


Fig. 3 CAD model of the mechanism

Table 1 Dimensions of the mechanism

Dimension	Value (mm)
Cylinder diameter	68
A	155.4
B_x	60
B_y	18
C_y	8
R	36
J	60
L	117.8
I	356.2

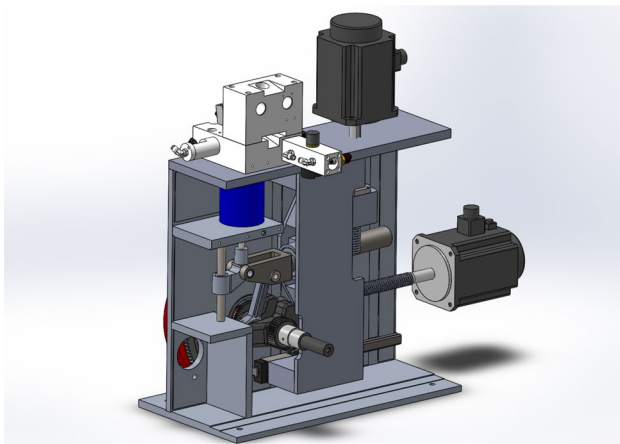


Fig. 4 Model of the prototype

optimized technological solution for mass production. A computational model of the prototype is shown in Fig. 4.

3 Kinematic model

The kinematics of the mechanism proposed in [5] is developed in this section. The equations are separated for the displacement, velocity, and acceleration. By implementing the analytical dynamics equations of motion [6], the nonlinear relations for the displacement can be seen in Sect. 3.1. This nonlinearity implies that it is opportune to fit a model into the region of interest to determine the pivot position given a set of compression ratio and cubic capacity. The following relations are given for the variables displayed in Figs. 5 and 6.

3.1 Displacement

Initially, we consider that the inertial referential is fixed with its origin coinciding with the crankshafts center of rotation. According to the nomenclature adopted here, the position of any point is represented by the vector w .

The angular position of the crankshaft is given by θ , and its radius is given by R . Hence, the position w_a (with respect to the inertial referential, which is considered to be fixed at the center of rotation of the crankshaft) is determined:

$$w_a = \begin{bmatrix} \cos \theta & -\sin \theta \\ \sin \theta & \cos \theta \end{bmatrix} \begin{Bmatrix} 0 \\ R \end{Bmatrix} = \begin{Bmatrix} -R \sin \theta \\ R \cos \theta \end{Bmatrix} \quad (1)$$

Similar to the conventional crank-rod mechanism, the connecting rod is pinned to the crank. Its length is considered to be L , and its inclination is given by γ , which gives us the position w_b :

$$w_b = w_a + \begin{bmatrix} \cos \gamma & -\sin \gamma \\ \sin \gamma & \cos \gamma \end{bmatrix} \begin{Bmatrix} 0 \\ L \end{Bmatrix} = \begin{Bmatrix} -R \sin \theta - L \sin \gamma \\ R \cos \theta + L \cos \gamma \end{Bmatrix} \quad (2)$$

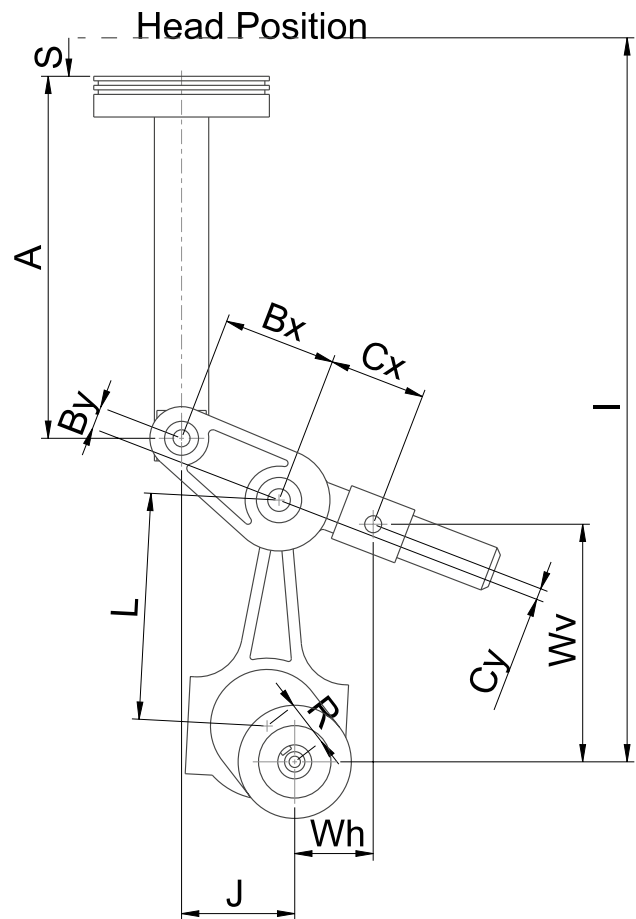


Fig. 5 Dimensions and variables of the kinematic model

The point at which the piston’s rod is connected moves according to the alternative displacement of the lever. By using the point b as the origin of the referential coordinate system, the position w_c is given by

$$w_c = w_b + \begin{bmatrix} \cos \alpha & -\sin \alpha \\ \sin \alpha & \cos \alpha \end{bmatrix} \begin{Bmatrix} -B_x \\ B_y \end{Bmatrix} = \begin{Bmatrix} -R \sin \theta - L \sin \gamma - B_x \cos \alpha - B_y \sin \alpha \\ R \cos \theta + L \cos \gamma - B_x \sin \alpha + B_y \cos \alpha \end{Bmatrix} \quad (3)$$

where B is the length of the lever’s left arm, and the position of point d is given by

$$w_d = w_c + \begin{Bmatrix} 0 \\ A \end{Bmatrix} = \begin{Bmatrix} -J \\ I - S \end{Bmatrix} \quad (4)$$

It should be noted that the piston executes a reciprocating movement in the vertical direction. Thus, the horizontal position can be used as a boundary condition for the solution of the equations.

$$-R \sin \theta - L \sin \gamma - B_x \cos \alpha - B_y \sin \alpha = -J \quad (5)$$

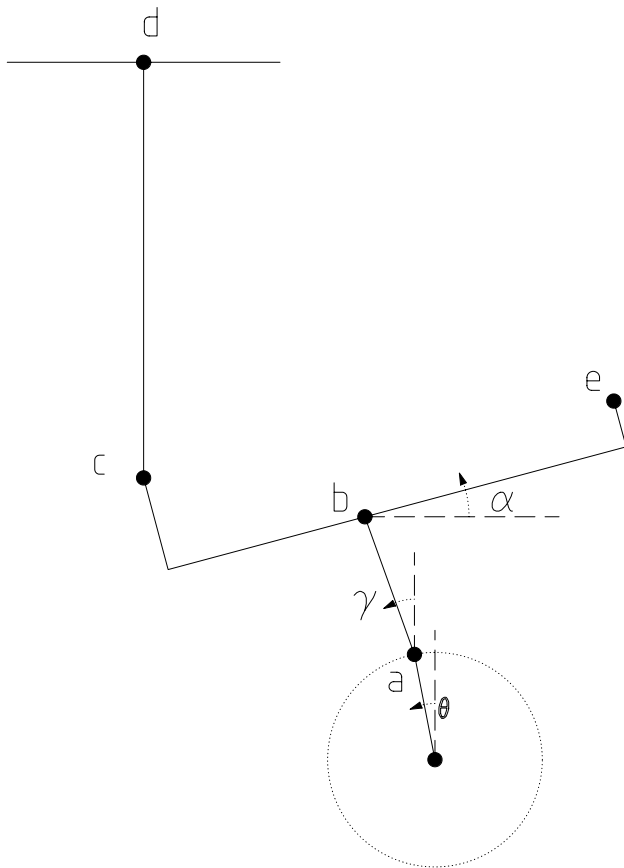


Fig. 6 Angles and points used in the analysis

Furthermore, the piston’s displacement S is given by

$$S = l - R \cos \theta - L \cos \gamma + B_x \sin \alpha - B_y \cos \alpha - A \tag{6}$$

The position of the piston determines the instantaneous volume V of the combustion chamber:

$$V = S \frac{\pi d_c^2}{4} \tag{7}$$

in which the diameter of the cylinder is represented by d_c .

The dislocated volume gives the cubic capacity (CC):

$$CC = [\max(S) - \min(S)] \frac{\pi d_c^2}{4} \tag{8}$$

and the compression ratio (CR):

$$CR = \frac{CC}{\min(S)} + 1 \tag{9}$$

There are three unknown variables: α , γ , and C_x . Therefore, it is necessary to obtain another two boundary conditions in order to solve the equations. The position of the pivot is defined by the actuation system and, as a result, is known.

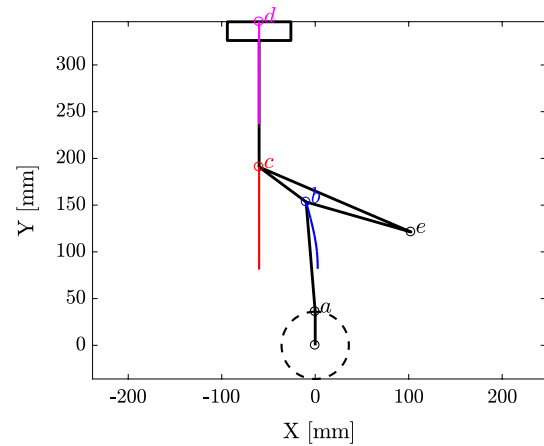


Fig. 7 Trajectory of each point at the maximum cubic capacity

The position of the pivot can be represented by w_e , which can be found as follows:

$$\begin{aligned} w_e &= w_b + \begin{bmatrix} \cos \alpha & -\sin \alpha \\ \sin \alpha & \cos \alpha \end{bmatrix} \begin{Bmatrix} C_x \\ C_y \end{Bmatrix} \\ &= \begin{Bmatrix} -R \sin \theta - L \sin \gamma + C_x \cos \alpha - C_y \sin \alpha \\ R \cos \theta + L \cos \gamma + C_x \sin \alpha + C_y \cos \alpha \end{Bmatrix} \end{aligned} \tag{10}$$

The above relation must represent the imposed position of the pivot; thus,

$$\begin{Bmatrix} -R \sin \theta - L \sin \gamma + C_x \cos \alpha - C_y \sin \alpha \\ R \cos \theta + L \cos \gamma + C_x \sin \alpha + C_y \cos \alpha \end{Bmatrix} = \begin{Bmatrix} W_h \\ W_v \end{Bmatrix} \tag{11}$$

As the unknown variables are trigonometric function’s arguments, an analytical solution cannot be easily found. Therefore, the system was solved numerically by implementing the Newton–Raphson method [4].

Figures 7 and 8 present the trajectory of each point for a full revolution of the crank, while Figs. 7 and 8 show the conditions of maximum and minimum cubic capacities, respectively.

The trajectory of d is shortened as e is positioned far from b as it can be perceived when comparing point c in Figs. 7 and 8.

3.2 Velocity

The velocity relations are derived by assuming that the crankshaft is rotating at a constant speed that is represented by $\dot{\theta}$. Thus, the velocity of point a is given by differentiating Eq. 1:

$$\dot{w}_a = \begin{Bmatrix} -\dot{\theta}R \cos \theta \\ -\dot{\theta}R \sin \theta \end{Bmatrix} \tag{12}$$

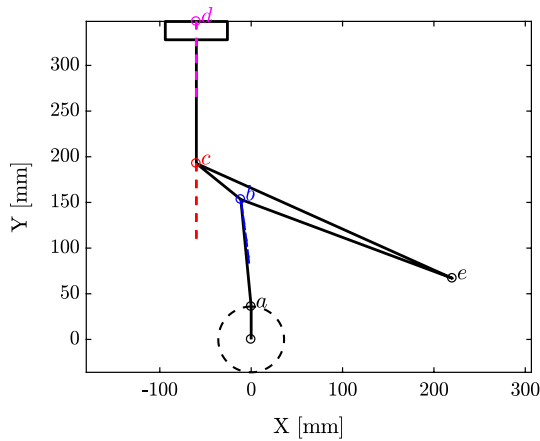


Fig. 8 Trajectory of each point at the minimum cubic capacity

Similarly, the velocity of point *b* is obtained by the differentiation Eq. 2:

$$\dot{\mathbf{w}}_b = \begin{Bmatrix} -\dot{\theta}R \cos \theta - \dot{\gamma}L \cos \gamma \\ -\dot{\theta}R \sin \theta - \dot{\gamma}L \sin \gamma \end{Bmatrix} \quad (13)$$

And for point *c*, Eq. 3 is differentiated, obtaining:

$$\dot{\mathbf{w}}_c = \begin{Bmatrix} 0 \\ -\dot{S} \end{Bmatrix} \quad (14)$$

As point *d* follows point *c*, their velocities are the same, i.e., $\dot{\mathbf{w}}_d = \dot{\mathbf{w}}_c$, and as the piston executes a reciprocating trajectory in the vertical direction, the horizontal component can be used as boundary condition:

As in the displacement model, there are three unknown variables—the angular velocities $\dot{\gamma}$ and $\dot{\alpha}$ and the rate of change in the arm length \dot{C}_x —and consequently, it is necessary to obtain three boundary conditions to solve the equations. As this study involves a mechanism operating at stable conditions, the pivot is assumed to be static, and thus, the velocity of the pivot is null.

$$\begin{aligned} \dot{\mathbf{w}}_e &= \begin{Bmatrix} -\dot{\theta}R \cos \theta - \dot{\gamma}L \cos \gamma - \dot{\alpha}C_x \sin \alpha - \dot{\alpha}C_y \cos \alpha + \dot{C}_x \cos \alpha \\ -\dot{\theta}R \sin \theta - \dot{\gamma}L \sin \gamma + \dot{\alpha}C_x \cos \alpha - \dot{\alpha}C_y \sin \alpha + \dot{C}_x \sin \alpha \end{Bmatrix} \\ &= \begin{Bmatrix} 0 \\ 0 \end{Bmatrix} \end{aligned} \quad (15)$$

The velocity of the piston is given by Eq. 14. It should be noted that this relation does not depend on \dot{C}_x . Therefore, using the boundary conditions given by Eqs. 14 and 15, it is possible to eliminate \dot{C}_x and define $\dot{\alpha}$ and $\dot{\gamma}$ using analytical expressions:

$$\dot{\alpha} = \frac{\dot{\theta}R \sin(\theta - \alpha) + \dot{\gamma}L \sin(\gamma - \alpha)}{C_x} \quad (16)$$

$$\dot{\gamma} = \frac{\dot{\theta}R \left(\frac{B_x \sin \alpha - B_y \cos \alpha}{C_x} \right) \sin(\theta - \alpha) - \cos \theta}{\cos \gamma - \left(\frac{B_x \sin \alpha - B_y \cos \alpha}{C_x} \right) \sin(\gamma - \alpha)} \quad (17)$$

\dot{C}_x is determined by using one of the relations given by Eq. 15:

$$\dot{C}_x = \frac{\dot{\theta}R \cos \theta + \dot{\gamma}L \cos \gamma + \dot{\alpha}(C_x \sin \alpha + C_y \cos \alpha)}{\cos \alpha} \quad (18)$$

It should be noted that any of the components of Eq. 15 could be used to determine \dot{C}_x . However, it was preferred to use the horizontal component as the relation obtained has $\cos \alpha$ as the denominator, and as α assumes values near zero, the equation is computationally stable.

3.3 Acceleration

As cited previously, this analysis is performed while considering the crankshaft to be rotating at a constant speed. By differentiating the relations of velocity found for each point, the following relations were derived:

$$\ddot{\mathbf{w}}_a = \begin{Bmatrix} \dot{\theta}^2 R \sin \theta \\ -\dot{\theta}^2 R \cos \theta \end{Bmatrix} \quad (19)$$

$$\ddot{\mathbf{w}}_b = \begin{Bmatrix} \dot{\theta}^2 R \sin \theta + \dot{\gamma}^2 L \sin \gamma - \ddot{\gamma} L \cos \gamma \\ -\dot{\theta}^2 R \cos \theta - \dot{\gamma}^2 L \cos \gamma - \ddot{\gamma} L \sin \gamma \end{Bmatrix} \quad (20)$$

$$\begin{aligned} \ddot{\mathbf{w}}_c &= \begin{Bmatrix} \dot{\theta}^2 R \sin \theta + \dot{\gamma}^2 L \sin \gamma - \ddot{\gamma} L \cos \gamma \\ -\dot{\theta}^2 R \cos \theta - \dot{\gamma}^2 L \cos \gamma - \ddot{\gamma} L \sin \gamma \\ +\dot{\alpha}^2(B_x \cos \alpha + B_y \sin \alpha) - \ddot{\alpha}(-B_x \sin \alpha + B_y \cos \alpha) \\ -\dot{\alpha}^2(-B_x \sin \alpha + B_y \cos \alpha) - \ddot{\alpha}(B_x \cos \alpha + B_y \sin \alpha) \end{Bmatrix} \end{aligned} \quad (21)$$

The above relation comprises the first boundary condition for solving the equations of acceleration as it represents the acceleration of the piston, of which the horizontal component is zero:

$$\ddot{\mathbf{w}}_c = \begin{Bmatrix} 0 \\ -\ddot{S} \end{Bmatrix} \quad (22)$$

In order to determine the remaining variables, the acceleration of point *e* is used again as a boundary condition:

$$\begin{aligned} \ddot{\mathbf{w}}_e &= \begin{Bmatrix} \dot{\theta}^2 R \sin \theta + \dot{\gamma}^2 L \sin \gamma - \ddot{\gamma} L \cos \gamma - \dot{\alpha}^2(C_x \cos \alpha - C_y \sin \alpha) \\ -\dot{\theta}^2 R \cos \theta - \dot{\gamma}^2 L \cos \gamma - \ddot{\gamma} L \sin \gamma - \dot{\alpha}^2(C_x \sin \alpha + C_y \cos \alpha) \\ -\dot{\alpha}(C_x \sin \alpha + C_y \cos \alpha) - 2\dot{\alpha}\dot{C}_x \sin \alpha + \ddot{C}_x \cos \alpha \\ +\dot{\alpha}(C_x \cos \alpha - C_y \sin \alpha) + 2\dot{\alpha}\dot{C}_x \cos \alpha + \ddot{C}_x \sin \alpha \end{Bmatrix} = \begin{Bmatrix} 0 \\ 0 \end{Bmatrix} \end{aligned} \quad (23)$$

The unknown variables are $\ddot{\alpha}$, $\ddot{\gamma}$, and \ddot{C}_x . On using the three given boundary conditions, we obtain

$$\ddot{\alpha} = \frac{\dot{\theta}^2 R \cos(\theta - \alpha) + \dot{\gamma}^2 L \cos(\gamma - \alpha) + \ddot{\gamma} L \sin(\gamma - \alpha) + \dot{\alpha}^2 C_y - 2\dot{\alpha}\dot{C}_x}{C_x} \tag{24}$$

$$\dot{\gamma} = \left\{ L \left[\cos \gamma + \frac{\sin(\gamma - \alpha)}{C_x} (-B_x \sin \alpha + B_y \cos \alpha) \right] \right\}^{-1} \left\{ \dot{\theta}^2 R \sin \theta + \dot{\gamma}^2 L \sin \gamma + \dot{\alpha}^2 (B_x \cos \alpha + B_y \sin \alpha) - \frac{(B_y \cos \alpha - B_x \sin \alpha)}{C_x} [\dot{\theta}^2 R \cos(\theta - \alpha) + \dot{\gamma}^2 L \cos(\gamma - \alpha) + \dot{\alpha}^2 C_y - 2\dot{\alpha}\dot{C}_x] \right\} \tag{25}$$

and the acceleration of the piston is given by Eq. 22.

4 Interpolation of the control parameters

A model for linking the cubic capacity and compression ratio to the position of the pivot is described in this section. In the previous sections, the need for developing such a relation was explained, as the relations of motion are not linear. Moreover, as a simulation of the engine performance would require the evaluation of the mechanisms operation

at several different conditions, *ad hoc* adjustments would not be convenient.

The adopted strategy comprised the mapping of the entire range of operation of the mechanism, while defining the compression ratio and cubic capacity of each pair of coordinates of the pivot, as shown in Fig. 9. The mechanism was set to operate with a cubic capacity going from 315 to 400 cm³ and a compression ratio going from 6:1 to 20:1.

However, it is desired to obtain the position of the pivot as a function of the cubic capacity and compression ratio instead of obtaining the cubic capacity and compression ratio as a function of the position of the pivot. Therefore, the coordinates were determined as a function of the engine parameters as shown in Fig. 10.

Although both components of the displacement influence both the cubic capacity and compression ratio, the horizontal component is strongly linked to the cubic capacity while the vertical component is strongly linked to the compression ratio. Thus, we opted to develop the following two expressions:

$$W_h = W_h(CC, CR) \rightarrow W_h(CC, f(CR)) \tag{26}$$

and

$$W_v = W_v(CR, CC) \rightarrow W_v(CR, f(CC)) \tag{27}$$

By performing regression, it was found that

$$W_h = A_{W_h} \exp \left(\frac{B_{W_h}}{CC} + \frac{C_{W_h}}{CC^2} \right) \tag{28}$$

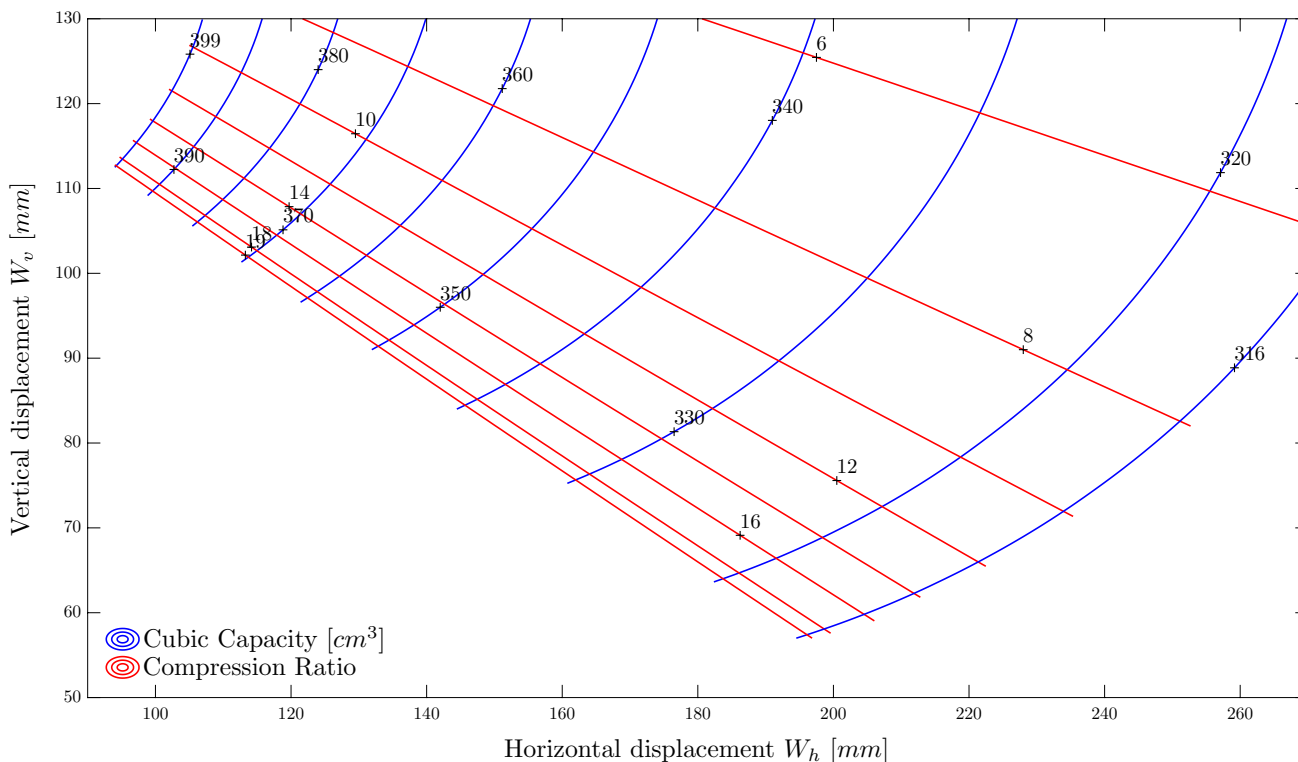


Fig. 9 Base map for interpolation

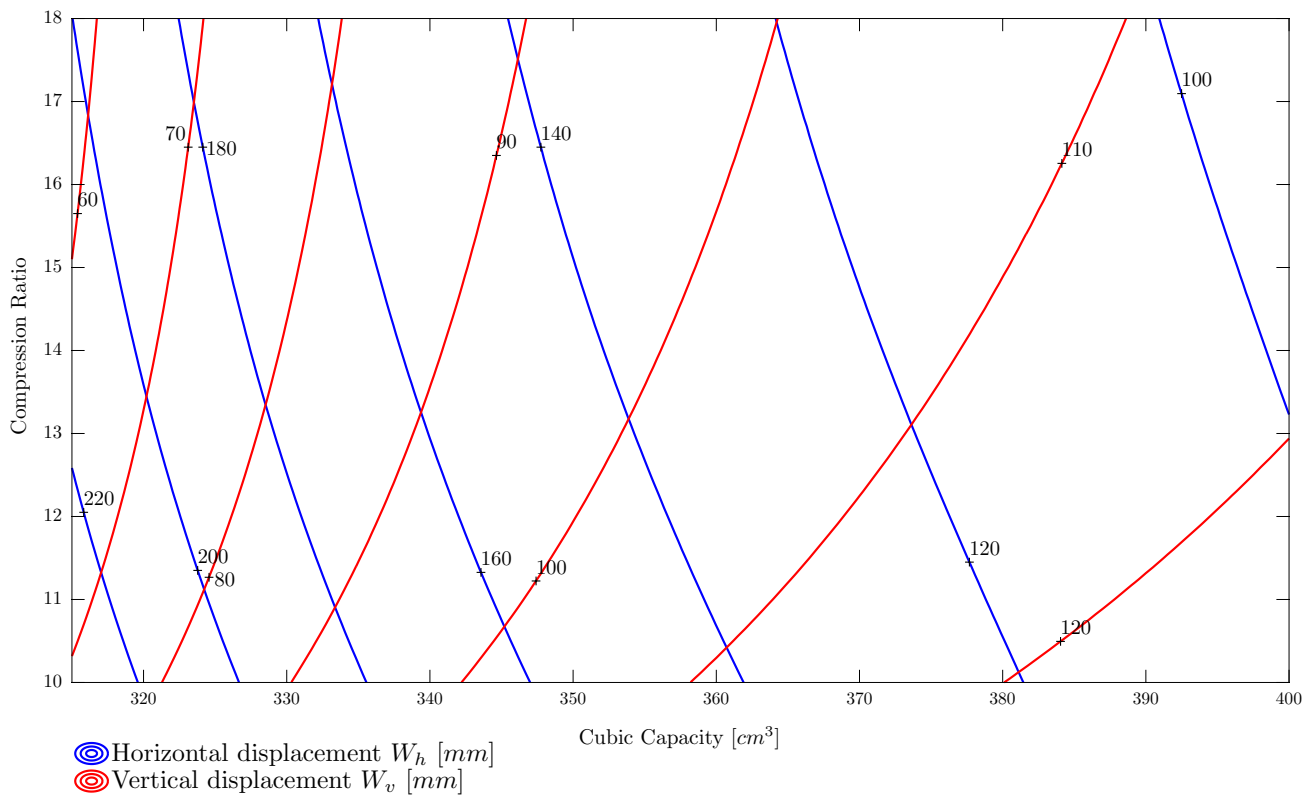


Fig. 10 Map for the position set of the pivot

wherein

$$A_{W_h} = \alpha_{A_{W_h}} + \beta_{A_{W_h}} \ln(\text{CR}) \tag{29}$$

$$C_{W_v} = \alpha_{C_{W_v}} + \frac{\beta_{C_{W_v}}}{\text{CC}} + \frac{\delta_{C_{W_v}}}{\text{CC}^2} \tag{35}$$

$$B_{W_h} = \alpha_{B_{W_h}} + \frac{\beta_{B_{W_h}}}{\text{CR}} + \frac{\delta_{B_{W_h}}}{\text{CR}^2} \tag{30}$$

$$C_{W_h} = \alpha_{C_{W_h}} + \beta_{C_{W_h}} \ln(\text{CR}) + \delta_{C_{W_h}} \ln^2(\text{CR}) \tag{31}$$

In the case of the vertical component, it was found that

$$W_v = A_{W_v} \exp\left(\frac{B_{W_v}}{\text{CR}} + \frac{C_{W_v}}{\text{CR}^2}\right) \tag{32}$$

wherein

$$A_{W_v} = \alpha_{A_{W_v}} + \beta_{A_{W_v}} \ln(\text{CC}) + \delta_{A_{W_v}} \ln^2(\text{CC}) \tag{33}$$

$$B_{W_v} = \alpha_{B_{W_v}} \exp\left(\frac{\beta_{B_{W_v}}}{\text{CC}} + \frac{\delta_{B_{W_v}}}{\text{CC}^2}\right) \tag{34}$$

The variables proposed were determined by the implementation of the least squares method, which resulted in the values presented in Table 2.

These relations represent an average percent deviation [10] of 0.44% for both W_h and W_v . It should be noted that there is a difference between the desired values of the compression ratio and cubic capacity and the effective values of both. On comparing the results obtained with the assigned values, an average percent deviation of 0.94% and 0.17% was found in the compression ratio and cubic capacity, respectively.

5 Results

The described model was implemented and run using Fortran code. The generated results were then loaded to the platform MATLAB to perform the analysis. This analysis comprises the verification of the desired characteristics mentioned in the previous sections, which is described in this section. The aforementioned desired characteristics

Table 2 Parameters of the interpolation

Parameter	Value
$\alpha_{A_{wh}}$	- 224.856647
$\beta_{A_{wh}}$	119.792433
$\alpha_{B_{wh}}$	- 1582.807539
$\beta_{B_{wh}}$	7892.012552
$\delta_{B_{wh}}$	39677.439377
$\alpha_{C_{wh}}$	- 821563.554214
$\beta_{C_{wh}}$	730561.355817
$\delta_{C_{wh}}$	- 110027.677793
$\alpha_{A_{wv}}$	- 23936.295463
$\beta_{A_{wv}}$	7977.219991
$\delta_{A_{wv}}$	- 661.899957
$\alpha_{B_{wv}}$	137589.999804
$\beta_{B_{wv}}$	- 7830.134472
$\delta_{B_{wv}}$	1380900.8319
$\alpha_{C_{wv}}$	89.819454
$\beta_{C_{wv}}$	- 78474.864516
$\delta_{C_{wv}}$	17192106.2599

are the stroke–bore ratio, effects of the cubic capacity and compression ratio variation on the kinematics, and a comparison with the kinematics of a conventional engine.

5.1 Stroke–bore ratio

As explained previously, a small stroke–bore ratio is undesirable as it decreases the engine efficiency. Thus, it is important to verify how the stroke–bore ratio varies with the cubic capacity for the configuration of the mechanism. The stroke length was calculated for each condition of the cubic capacity (it should be noted that this parameter does not depend on the compression ratio) and is shown in Fig. 11.

The components of the mechanism were designed in a manner such that the stroke length–bore ratio would not be less than 1 for the entire range of the cubic capacity, as can be verified in Fig. 12:

It is mentioned in [9] that the effects of heat transfer and flame speed are only observed in small values of the stroke–bore ratio (less than 0.5). Therefore, we do not expect to find that the efficiency decreases with a reduction of the stroke length.

5.2 Influence of compression ratio on kinematics

In Fig. 13, how the position profile of the piston behaves as the compression ratio varies is shown. The increase in the clearance volume with the decrease in the compression ratio and how this relation is nonlinear is highlighted.

The displacement profile practically suffers no modification with a variation in the compression ratio (Fig. 13). The

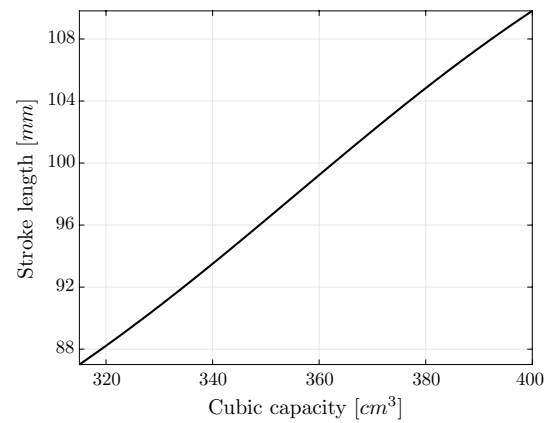


Fig. 11 Stroke length as a function of the cubic capacity

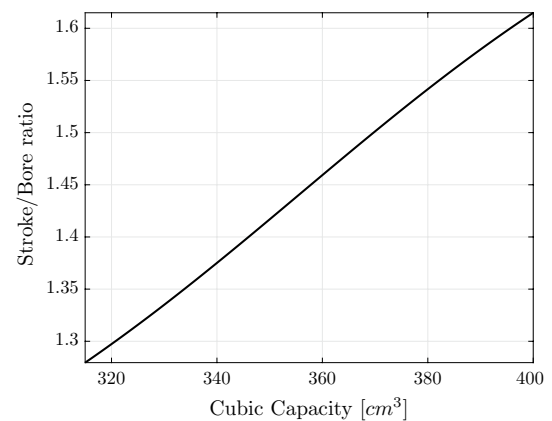


Fig. 12 Stroke length–bore ratio

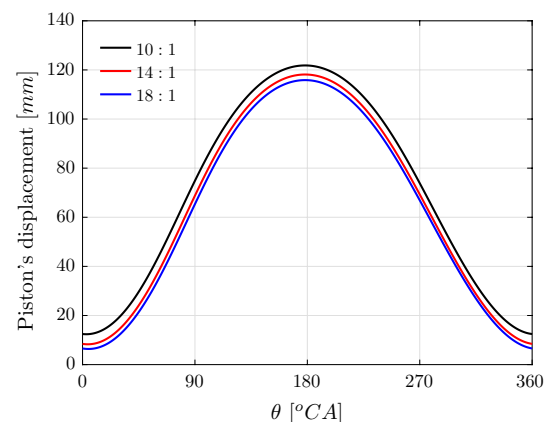


Fig. 13 Effect of the compression ratio on the position profile of the piston

adjustment of compression ratio is performed by altering the inclination of the lever. This causes a shift in the TDC and BDC, which is explained in Sect. 5.4.

5.3 Influence of cubic capacity on kinematics

The increase in the stroke length is accompanied by the increase in the cubic capacity as stated by Eq. 8 and illustrated in Fig. 14. Another aspect of the displacement when the cubic capacity is adjusted is the position of the TDC (Fig. 14). A variation in the position of the TDC occurs whenever the cubic capacity is set without changing the compression ratio. This occurs because the compression ratio is given by the ratio of the maximum and minimum (clearance volume) volumes of the combustion chamber. If the dislocated volume is changed, the clearance volume must vary in order to maintain a constant ratio (12:1 in the case of Fig. 14). This feature is a great disadvantage in VSE mechanisms, which only allow the adjustment of the stroke length. In such cases, it is impossible to adjust the cubic capacity by maintaining a constant compression ratio.

The variation in the cubic capacity affects the velocity profile by increasing its amplitude as the cubic capacity increases. This occurs because the lengthening of the stroke requires a higher velocity for the piston to run its stroke in the same period of time (see Fig. 15). Moreover, the position of the pivot affects the motion of the lever, thus changing the position of the velocity peak to approximately 90° CA (crank angle degree). Figures 15 and 16 were generated at an engine speed of 3500 rpm. The effect of the engine speed is only related to the amplitudes of both the velocity and acceleration. Thus, the effects on the profiles will be same irrespective of the engine speed.

As in the case of the velocity profile, significant changes are not observed in the acceleration profile with a reduction in the stroke length except in the case of a decrease in amplitude (see Fig. 16).

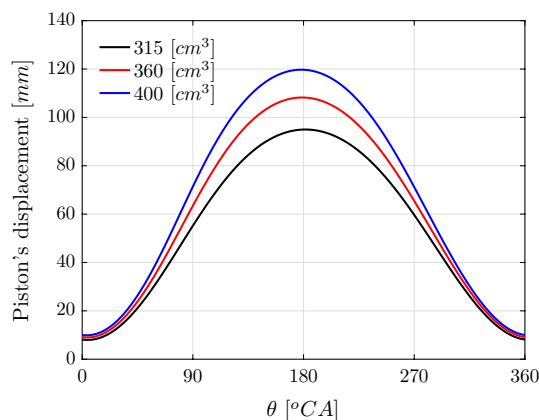


Fig. 14 Displacement profile of the piston

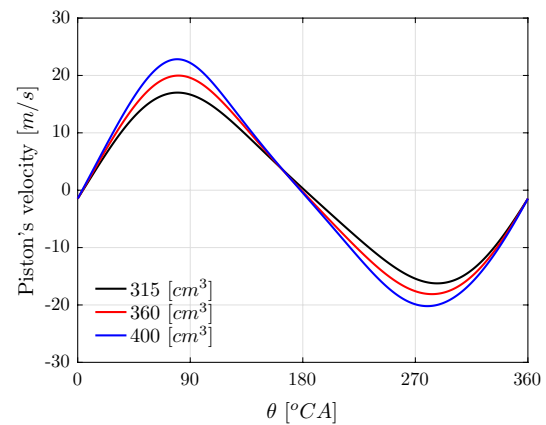


Fig. 15 Velocity profile of the piston

5.4 Phase shift of TDC and BDC

The nature of the trajectory of the components, mainly the inclination of the lever, creates a phase shift in the TDC and BDC. In Figs. 7 and 8, it is shown that the mechanism is static at $\theta = 0^\circ$ CA, and it is observed that the connecting rod is slightly tilted, which means that the TDC does not occur at exactly $\theta = 0^\circ$ CA nor does the BDC center occur at $\theta = 180^\circ$ CA. On comparing both figures, it is noted that the TDC and BDC positions depend on the configuration of the mechanism. For the entire range of the compression ratio and cubic capacity, the phase shifts in the TDC and BDC were calculated and mapped. The obtained results are presented in Figs. 17 and 18.

The phase shift in the TDC is strongly related to the compression ratio, which assumes values from $+3^\circ$ to $+5.2^\circ$ and is always positive. In contrast, it is verified that the phase shift of the BDC is almost symmetrical and varies from -1.5° to $+2^\circ$; it is strongly dependent on the cubic capacity.

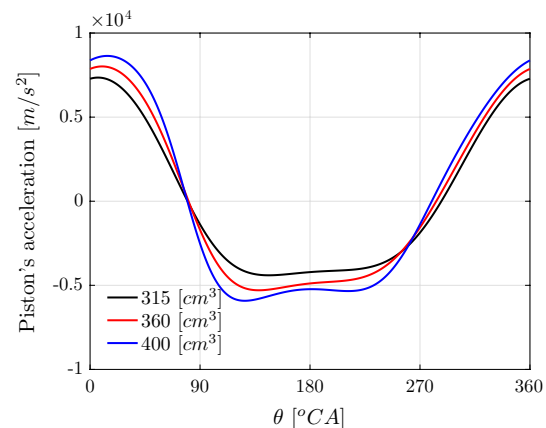


Fig. 16 Acceleration profile of the piston

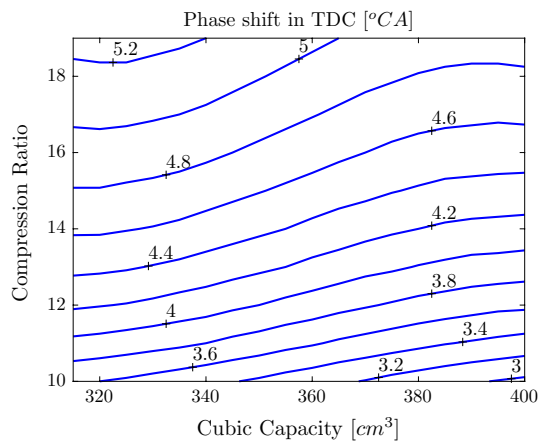


Fig. 17 Phase shift in TDC

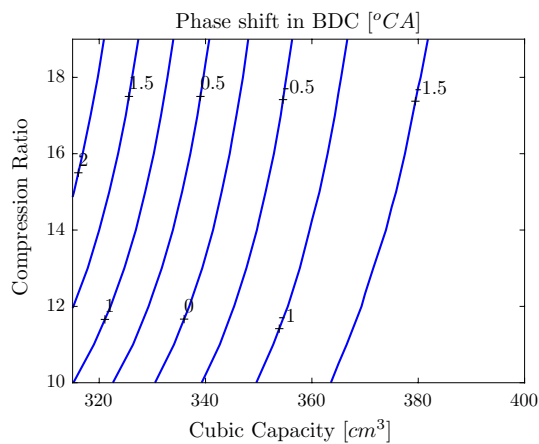


Fig. 18 Phase shift in BDC

This phase shift is not to be considered as a drawback as the ECU can be easily calibrated to identify the shift and correct events that are dependent on the TDC and BDC, such as the spark advance. Even if the engine does not allow the control of the valve phasing, the magnitude of the phase shift in the TDC and BDC would not harm the gas exchange process. This effect of the phase shift is already observed when a conventional crank-rod mechanism presents an eccentricity, i.e., when the axis of the cylinder is not aligned with the crankshaft axis in order to minimize the lateral forces acting on the piston’s head.

5.5 Comparison with the conventional mechanism

One of the main concerns in the design of the proposed mechanism is to preserve the kinematics characteristics observed in a conventional crank-rod mechanism. Therefore,

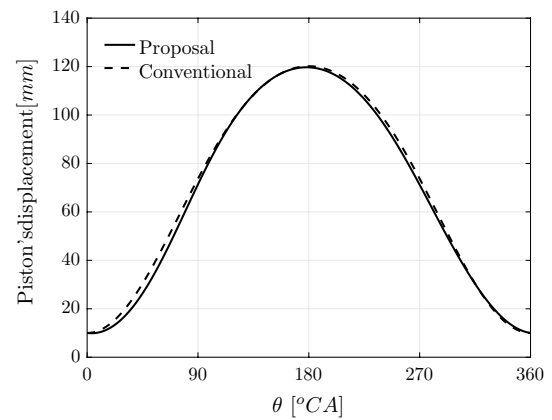


Fig. 19 Comparison of the position profile between the proposed engine and a conventional engine

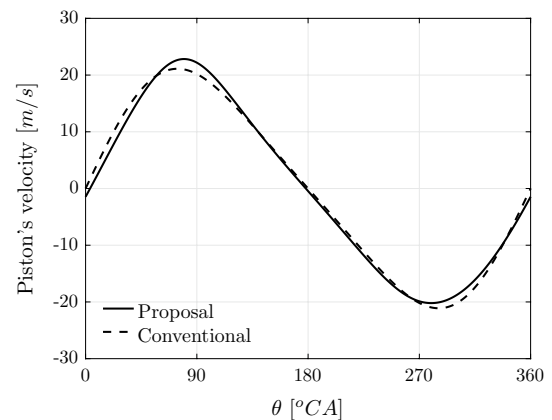


Fig. 20 Comparison of the velocity profile between the proposed engine and a conventional engine

the kinematics of a conventional mechanism was simulated with the same cubic capacity as that of the proposed mechanism in the simulated condition. As the crank radius is greater in a conventional engine for reasons explained in Sect. 2, the connecting rod of the simulated model was increased in order to maintain the same ratio of rod length to crank radius.

The profiles of the displacement, velocity, and acceleration are given in Figs. 19, 20, and 21, respectively.

There is a slight difference between the kinematics of a conventional engine and the proposed one (Figs. 19, 20, and 21). It is verified in Fig. 21 that the acceleration profile is symmetrical in the conventional engine, whereas in the proposed mechanism it is slightly asymmetrical. For all conditions of cubic capacity and compression ratio, this difference was evaluated. However, a characteristic to be considered in this analysis is the variation of the maximum amplitude between the conventional and proposed mechanisms, which is small.

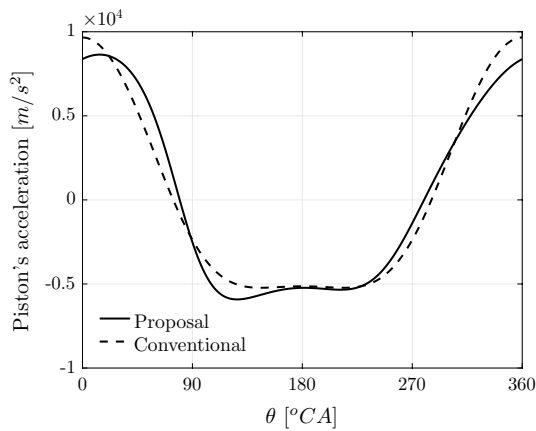


Fig. 21 Comparison of the acceleration profile between the proposed engine and a conventional engine

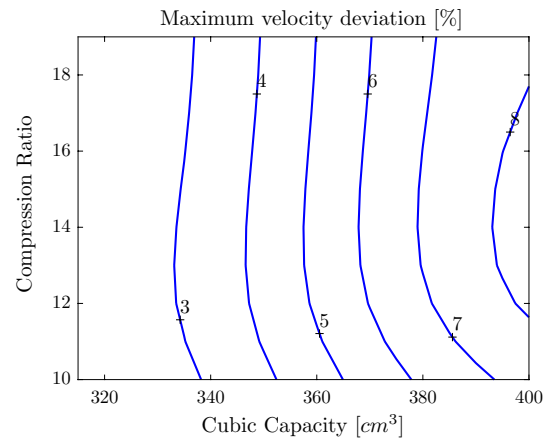


Fig. 23 Maximum velocity deviation

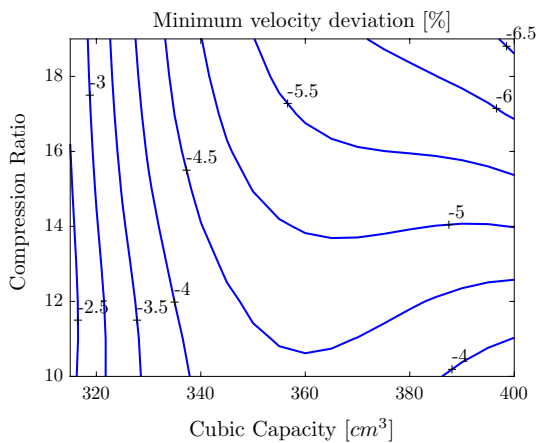


Fig. 22 Minimum velocity deviation

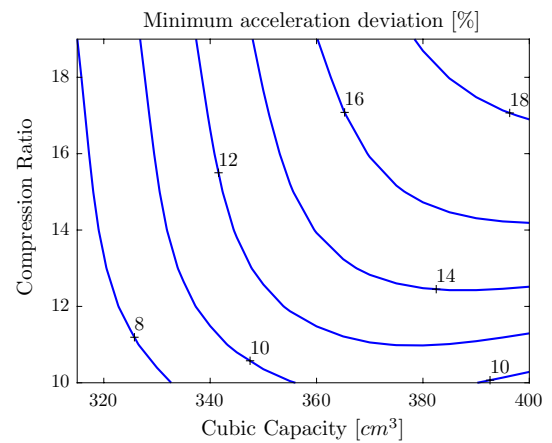


Fig. 24 Minimum acceleration deviation

At a large cubic capacity, the compression ratio has a strong relation with the minimum velocity (see Fig. 22). This occurs because of the inclination of the lever in that specific condition. For small values of cubic capacity, the velocity is almost independent of the compression ratio. For all conditions, the compression ratio has little or no influence on the velocity (Fig. 23). It is thus concluded that the mechanism reduces the maximum velocity in the trajectory from the BDC to TDC (negative values) while it increases the maximum velocity along the trajectory from the TDC to BDC (positive values). In addition, the maximum absolute deviation found was 8%. Similar effects were verified with respect to the acceleration; its maximum value for the BDC-to-TDC trajectory is presented in Fig. 24, and its maximum value for the TDC-to-BDC trajectory is presented in Fig. 25.

A large deviation is observed in the acceleration as compared to the velocity. Nevertheless, the maximum deviation is less than 20%. To our understanding, these results present

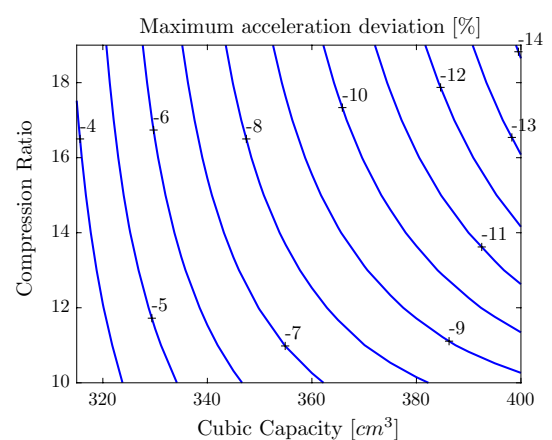


Fig. 25 Maximum acceleration deviation

effects that are not expected to significantly influence the engine performance.

6 Conclusions

Variable stroke and compression ratio engines have been studied in the recent years as a potential to provide a significant improvement in efficiency and reduction in pollutant emissions. In order to evaluate the impact that such technology would have on the automotive sector, research and extensive tests have been conducted. One of the first tasks in this direction is to study the kinematic behavior of the engine. Based on the kinematics, it is possible to evaluate the features of the technology. Moreover, the study of the kinematics provides fundamental information that is required for the dynamics evaluation and design of components, as it provides information that is required for a performance analysis through a phenomenological, i.e., thermodynamic, simulation. This work presents the kinematic study of a VSE mechanism proposed in [5] and also involved the development of tools for determining the engines operational configuration (in this case, the position of the pivot) according to the desired set of cubic capacity and compression ratio values.

Subsequent to the development of the described tools, some requirements for the implementation of the mechanism were evaluated. The obtained results showed that the mechanism meets the established requirements of independent adjustment of stroke length and compression ratio. It is possible to control the stroke length in a significant range from 315 to 400 cm³, with the possibility of redesign that results in a greater range. On the other hand, the compression ratio range is very flexible with the same actuator. Although the configuration studied ranges from 6:1 to 20:1, it is possible to achieve higher compression ratios with the same solution without any system recalculation. The preservation of the motion obtained in a conventional crank-rod mechanism is another requirement that was satisfactorily met.

The work presented in this paper provides a basis for future studies that could quantify the impact of the implementation of such technology in the transportation sector. Prospective research will use the developed model to perform simulations on engine performance and emissions as well as for design and structural analysis purposes.

Acknowledgements The authors would like to express their gratitude to the Fundação de Amparo à Pesquisa do Estado de São Paulo (FAPESP) for the support provided through process no 2016/06043-1, a research part of the research center “Prof. Urbano Ernesto Stumpf” (process no 2013/50238-3), and to PSA Peugeot for the financial and technical support provided.

References

1. Elkholy AH (1995) Variable stroke piston mechanism for spark ignition engines. *Int J Veh Design* 16(6):570–580
2. Ferreira JV, Rufino CH (2014) Motor de combusto interna com mecanismo que permite controle instantaneo sobre a taxa de compresso e a capacidade volumetrica de cada cilindro individualmente e seus usos. Patent INPI BR 10 2014 026240 7
3. Heywood J, MacKenzie D (2015) On the road toward 2050: potential for substantial reductions in light-duty vehicle energy use and greenhouse gas emissions. Massachusetts Institute of Technology
4. Press WH (2007) Numerical recipes 3rd edition: the art of scientific computing. Cambridge University Press, Cambridge
5. Rufino CH, Ferreira JV (2017) Adjustable stroke length and compression ratio engine. *Acta Mechanica et Mobilitatem* 2(3):1–11
6. Schiehlen W, Eberhard P (1986) Technische dynamik. Springer, Berlin
7. Shaik A, Moorthi NV, Rundramoorthy R (2007) Variable compression ratio engine: a future power plant for automobiles—an overview. In: Proc. IMechE part D: automobile engineering, p 221
8. Siegl DC, Siewert RM (1978) The variable stroke engine—problems and promises. SAE Technical Paper No 780700
9. Siewert RC (1978) Engine combustion at large bore-to-stroke ratios. SAE Technical Paper No 780968
10. Stoecker WF (1980) Design of thermal systems. McGraw Hill Book Company, New York
11. Walter A, Dolzan P, Quilodrán O, de Oliveira JG, da Silva C, Piacente F, Segerstedt A (2011) Sustainability assessment of bio-ethanol production in Brazil considering land use change, GHG emissions and socio-economic aspects. *Energy Policy* 39(10):5703–5716